


Article

Impact of Pulse Disturbances on Phytoplankton: How Four Storms of Varying Magnitude, Duration, and Timing Altered Community Responses

Noah Claflin ¹, Jamie L. Steichen ¹, Darren Henrichs ² and Antonietta Quigg ^{1,2,*}

¹ Department of Marine Biology, Texas A & M University at Galveston, Galveston, TX 77553, USA; nclaflin27@tamu.edu (N.C.); jamie.steichen@tamu.edu (J.L.S.)

² Department of Oceanography, Texas A & M University, College Station, TX 77854, USA; dhenrichs@tamu.edu

* Correspondence: quigga@tamug.edu; Tel.: +1-409-740-4990

Abstract: Estuarine phytoplankton communities are acclimated to environmental parameters that change seasonally. With climate change, they are having to respond to extreme weather events that create dramatic alterations to ecosystem function(s) on the scale of days. Herein, we examined the short term (<1 month) shifts in phytoplankton communities associated with four pulse disturbances (Tax Day Flood in 2016, Hurricane Harvey in 2017, Tropical Storm Imelda in 2019, and Winter Storm Uri in 2021) that occurred in Galveston Bay (TX, USA). Water samples collected daily were processed using an Imaging FlowCytobot (IFCB), along with concurrent measurements of temperature, salinity, and chlorophyll-a. Stronger storm events with localized heavy precipitation and flooding had greater impacts on community composition, increasing diversity (Shannon–Weiner and Simpson Indices) while a cold wave event lowered it. Diatoms and dinoflagellates accounted for the largest fraction of the community, cyanobacteria and chlorophytes varied mostly with salinity, while euglenoids, cryptophytes, and raphidophytes, albeit at lower densities, fluctuated greatly. The unconstrained variance of the redundancy analysis models pointed to additional environmental processes than those measured being responsible for the changes observed. These findings provide insights into the impact of pulse disturbances of different magnitudes, durations, and timings on phytoplankton communities.



Citation: Claflin, N.; Steichen, J.L.; Henrichs, D.; Quigg, A. Impact of Pulse Disturbances on Phytoplankton: How Four Storms of Varying Magnitude, Duration, and Timing Altered Community Responses. *Environments* **2024**, *11*, 218. <https://doi.org/10.3390/environments11100218>

Received: 6 August 2024

Revised: 13 September 2024

Accepted: 29 September 2024

Published: 4 October 2024



Copyright: © 2024 by the authors. Licensee MDPI, Basel, Switzerland. This article is an open access article distributed under the terms and conditions of the Creative Commons Attribution (CC BY) license (<https://creativecommons.org/licenses/by/4.0/>).

Keywords: extreme event; hurricane; cold wave; Imaging FlowCytobot; community composition

1. Introduction

Phytoplankton play a vital role as primary producers in freshwater, estuarine, and marine ecosystems [1]. Estuaries support high primary productivity and phytoplankton diversity, in part due to organic carbon and nutrient input from terrestrial sources [2,3]. Changes in water quality parameters, caused by anthropogenic or natural sources, can have significant effects on phytoplankton community structure [4]. In some cases, such as nutrient enrichment, this elicits blooms, some of which may be harmful or toxic to both the surrounding fauna and humans [5]. The distribution of phytoplankton is mostly governed by geographic region, water quality parameters such as temperature and salinity, and light availability and nutrient enrichment [6–9]. Phytoplankton communities have been the focus of many recent ecological studies concerning estuarine systems due to ongoing changes caused by biotic and abiotic factors [10–12]. With climate change, phytoplankton are also having to respond to dramatic alterations in ecosystems which occur during pulse disturbances [13] associated with extreme weather events such as storms, floods, or cold-wave events. Their response ultimately depends on both the characteristics of a particular storm and the physical–chemical conditions of the water column before the storm’s passage [14–17]. Concerns are increasing for estuaries that are experiencing an increased frequency in pulse disturbances (e.g., [18]).

The composition of phytoplankton communities in estuaries are important indicators of ecosystem health [19]. Ochrophyta (Bacillariophyceae; diatoms), Dinophyta (dinoflagellates), and Cyanophyta (cyanobacteria) are the most abundant groups of phytoplankton in estuaries and coastal zones [4,20–22]. Other prominent groups include Cryptophyta, Euglenophyta, and less so, Chlorophyta, Haptophyta, and Raphidophyta. Each of these groups have different ranges of water quality parameters (temperature, salinity, etc.) for optimal growth [23]. Monitoring changes in water quality parameters against changes in phytoplankton community is a critical step in determining how bays and estuaries may be changing over time. Prior studies examining phytoplankton community dynamics have used a variety of approaches including microscopy [24–26], photopigment analysis (e.g., [4,7,8]), and more recently, genetic analysis (e.g., [27]), with each method having its benefits and drawbacks. Photopigment analysis can only be used to distinguish phytoplankton groups to the taxa level (diatoms, dinoflagellates), while microscopy allows species level analysis but has associated extensive costs and work hours, while the genetic analysis often is still limited by the many “unknowns” in the databases. High-throughput sequencing and metabarcoding technology is providing valuable information about small (<10 μm) phytoplankton which are difficult to discern using most methods, including traditional flow cytometry. None of these tools are, however, practical for long-term monitoring or daily measurements. The Imaging FlowCytobot (IFCB) is the latest in a series of tools developed for continuous monitoring of phytoplankton community structure [28,29]. Flow cytometry has been demonstrated as an effective analysis technique in phytoplankton research [30]. Previously developed flow cytometers such as the FlowCAM [31] and the CytoSub [32] do not have the field endurance and resolution for prolonged, high-resolution ecological studies [28]. The IFCB has a demonstrated ability to effectively sample cells in the 10–100 μm size range, a critical group comprising many diatoms and dinoflagellates [15,33–36]. Nonetheless, it too has its drawbacks, including the challenges of building classifiers which effectively identify all members of the community within the size window of its flow cell.

When responding to extreme weather events, both people and instruments are important assets. In the current study, we explored IFCB and concurrently collected water quality data (salinity, temperature, and chlorophyll) to examine short term (<1-month post-storm) phytoplankton responses to four storms of varying magnitude, duration, and timing that hit Galveston Bay (TX, USA) between 2016 and 2021. Herein, we examined data for the Tax Day Flood in 2016, Hurricane Harvey in 2017, Tropical Storm Imelda in 2019, and Winter Storm Uri in 2021 (Table 1). Other major storm events during the study period include the Texas–Oklahoma Flood and Tornado Outbreak in 2015 and the Independence Day Flooding in 2018, but these were not included herein [see [37,38] for details of these storms]. The sampling presented herein was collected at one fixed location (Figure 1) as part of a long-term monitoring program. Concurrent physiochemical data (e.g., nutrients) are not available. Tropical storms and hurricanes are not uncommon in this region [3,14,27,39]. Within the context of global change, cold waves characterized by rapid cooling, leading to a rapid sea surface temperature or air temperature decrease in estuaries [40,41], are now becoming more common in this region. This study provides new insights into the potential impacts of future climate events on estuarine ecosystems, particularly the relationships governing phytoplankton community structure. These findings provide insights into the impact of pulse disturbance events of different magnitude, duration, and timing on phytoplankton communities examined using an IFCB.

Table 1. Major storm events examined with information on duration and pre- and post-storm periods.

	Tax Day Flood	Hurricane Harvey Category 4	Tropical Storm Imelda	Winter Storm Uri
Year	2016	2017	2019	2021
Dates	April 18	August 27–September 2	September 17–19	February 11–20
Season *	Spring	Summer	Fall	Winter

Table 1. *Cont.*

	Tax Day Flood	Hurricane Harvey Category 4	Tropical Storm Imelda	Winter Storm Uri
Precipitation (cm) at sampling site **	1.4	40	28.6	2.6
Precipitation (cm) in Houston	43	>76	25–30	1–3
Precipitation (cm) along Houston-Galveston corridor	15–30, up to 60 in some areas	50–76	>76	1–5
For RDA, pre-storm period	4/1–4/17	8/1–8/31	9/1–9/17	2/1–2/15
For RDA, post-storm period	4/18–5/4	9/1–9/29	9/18–9/30	2/6–3/7
Alternative name, if used in literature	North American Storm Complex			Texas Freeze

* In Galveston Bay, winter occurs from December to February, spring from March to May, summer from June to August, and fall (or autumn) from September to November. ** As measured at the nearby Scholes Airport, Galveston, TX, USA.

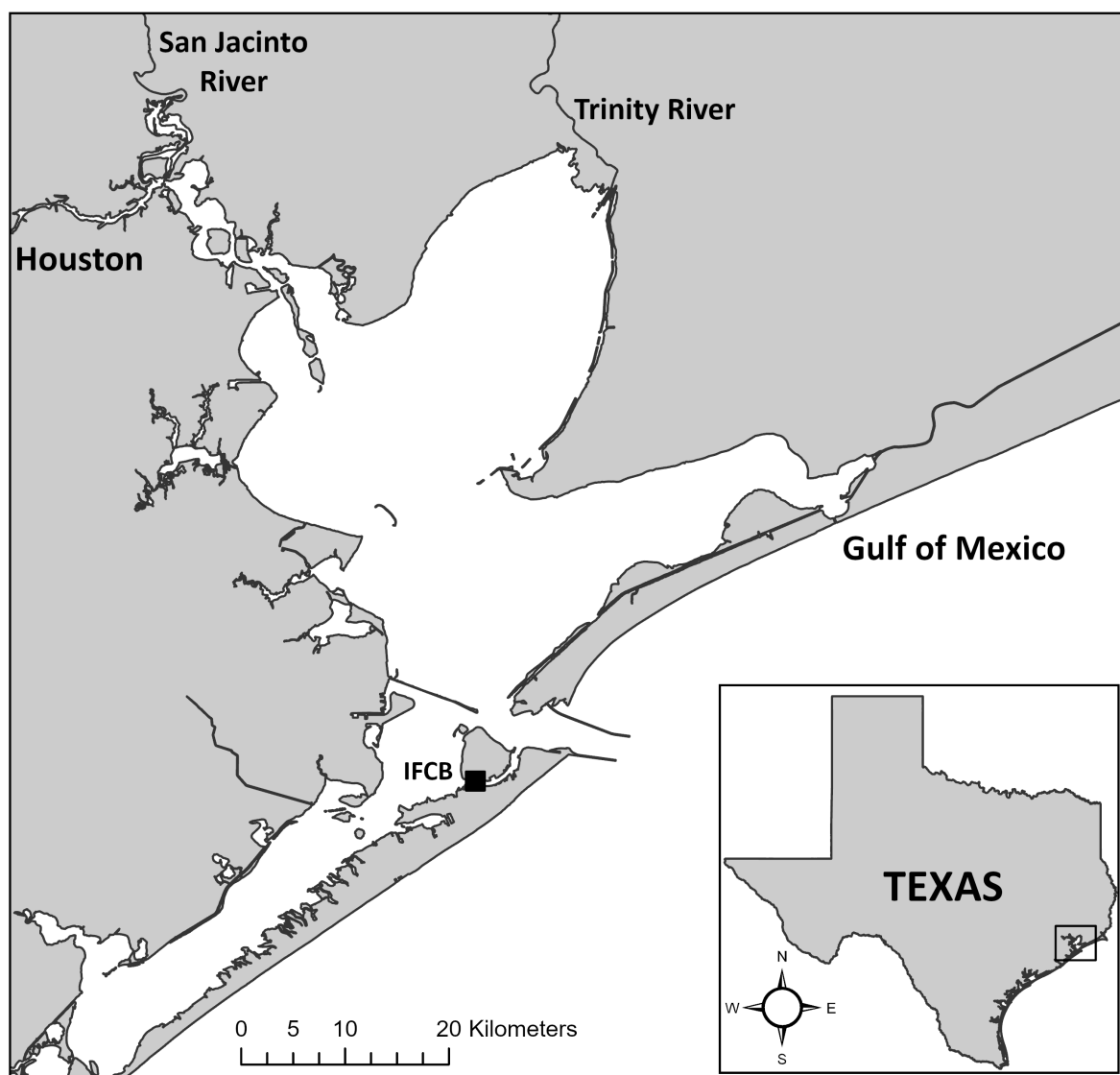


Figure 1. Galveston Bay, Texas located in the northwestern Gulf of Mexico. The IFCB samples and water quality data were collected from the marina located on the Texas A&M University at Galveston Campus.

2. Materials and Methods

2.1. Study Site and Sampling Station

Galveston Bay (Figure 1), also known as the Trinity–San Jacinto estuary, is ecologically and economically one of the most important systems for the Texas coast and the Gulf of Mexico [42]. Galveston Bay is the sixth largest estuary in the United States (1554 km²), and second largest in the northern Gulf of Mexico. This subtropical estuary located in a watershed covering over 64,000 km² [43] is often affected by tropical storms and hurricanes [4,8,44]. The excessive precipitation loads excess inorganic nutrients and suspended particulates into rivers upstream, impacting the estuary [45], and reshaping the phytoplankton community. In addition, Galveston Bay has recently experienced record-breaking low air temperatures in winter, including a super-cold wave in the 2020/2021 La Niña winter.

All subsurface (>0.30 to 100 cm) samples were collected in the small boat basin of the Texas A & M University at Galveston campus (29°18' N, 94°49' W) (Figure 1). This location was chosen to sample phytoplankton communities moving in and out of the bay from the Gulf of Mexico. It is at the point furthest from the main riverine inputs into the bay. Sampling started April 2015 and has continued daily except on occasions when the

instrument had to be shut down for repairs, or when the campus was closed or inaccessible due to evacuations for storms, flooding, and other severe weather.

2.2. Major Storm Events

We examined four storms of varying magnitude, duration, and timing which hit Galveston Bay (TX, USA) including the Tax Day Flood (2016), Hurricane Harvey (2017), Tropical Storm Imelda (2019) and Winter Storm Uri (2021) (Table 1). The first three of the events examined were associated with severe winds (hurricanes, tropical storms) or floods, while the fourth event involved the freeze event associated with snow and sleet. Information on the duration and type of storm was collected from the NOAA National Weather Service ([weather.gov](https://www.weather.gov), accessed on 18 January 2023) and summarized in Table 1. Study periods used in this analysis for the major storms examined begin around 15 to 30 days prior to, and after, the event (Table 1). Storm study periods were split into pre- and post-storm periods based on whichever of the following criteria were met first: five days after the start of the storm event, the end of the storm event, or the first day of sampling following the storm event. Broader periods were examined in an earlier analysis of these storms [38]; we found these shorter periods improved the model results (see below).

2.3. Sample and Environmental Data Collection

Daily water samples and environmental data were collected from the sampling station between 09:00 and 10:30 Central Standard Time. Water samples were collected into an opaque acid washed and triple rinsed bottle. Chlorophyll (chl)-a concentration was measured as a proxy for phytoplankton biomass using the procedure of Arar and Collins [46]. Briefly, cells were filtered under low vacuum (<130 Kpa) onto GF/F glass microfibre filters and frozen at -20°C . After extraction in 5 mL of 40:6:54 acetone/deionized water/dimethyl-sulfoxide solution for ~24 h in low light and low temperature, samples were mixed thoroughly by vortex, centrifuged at 2500 rpm (5 min), and the supernatant analyzed using a Turner 10AU Fluorometer (SN: 00239900). Each sample was then acidified using a dilute HCl solution, and chl-a concentrations calculated after correcting for phaeophytin. Salinity (reported on the unitless practical salinity scale) and temperature ($^{\circ}\text{C}$) were measured using a calibrated MS5 Hydrolab water quality sonde (SN: 160500067114) with a Hydras 3 LT (CN: 6234218). Local precipitation data were collected from Scholes International Airport (Galveston) from the NOAA National Centers for Environmental Information (NCEI) ([ncei.noaa.gov](https://www.ncei.noaa.gov), accessed on 1 February 2023) database.

2.4. IFCB

Within hours of collection, 5 mL increments of the homogenized water samples were run through the IFCB (McLane Research Laboratories). The IFCB captures images when chl-a fluorescence is detected in particles from 10 to 100 μm [28,29]. The sample water is pulled into the IFCB through a 130 μm pre-filter to remove large particles and debris. The sample is then passed through a red laser to detect the presence of chl-a in particles (e.g., phytoplankton cells). If chl-a fluorescence is detected, an image is captured and an onboard 'blob' analysis algorithm selects the region in each frame containing particles of interest. All images from an aliquot are saved along with associated metadata for the image (e.g., chl-a fluorescence, side-scatter). For a detailed description of the analytical system, please refer to Olson and Sosik [28]. Additional 5 mL aliquots are run until at least 200 phytoplankton cell images per daily sample are captured.

More than 90 categories (Table S1) of morphologically distinct phytoplankton, zooplankton, and 'other' material were classified using protocols of Sosik and Olson [29]. Each 'category' is a phytoplankton group, genus, or species. When clear identification was not possible, a descriptive name (e.g., round flagellate cells, chain forming diatoms) was used. Manual identification was required to compile and sort at least 100 images per category to train the classifier in image recognition [47,48]. Herein, we only considered those categories

created for phytoplankton and those in which we could assign a taxonomic classification (e.g., unknown dinoflagellate was included, small balls were excluded).

For each sample, images were extracted into a single file using MATLAB software package (version 7.2; Mathworks, Inc., Natick, MA, USA) and the associated Image Processing Toolbox (version 5.2; Mathworks, Inc.) (<https://github.com/hsosik/ifcb-analysis>, accessed on 18 October 2021). The Digital Image Processing Using MATLAB (DIPUM) toolbox (version 1.1.3; imageprocessingplace.com, accessed on 18 October 2021) processed images and a random forest classifier (MATLAB `treebagger` function; [49] was trained. The overall classification error rate for the IFCB classifier was 34% with 35% of images placed in an unclassified category. Images are considered unclassified if they did not meet the threshold required to place them into a category. The random forest classifier “optimum” output has the most stringent threshold for image classification and was used in this study. Application of the optimum classification threshold, resulting in a lowering of the overall error rate to 15%. Unclassified images were excluded from further analysis. Error rates for individual categories can vary and are often related to the cell shape and size (e.g., large diatoms are more easily identified while smaller, round cells are not).

2.5. Diversity Analysis

Ecological diversity metrics were calculated using the classified IFCB categories (cells/mL) according to Krebs [50] and separated into pre- and post-storm periods. Species richness (d) was used to determine the number of phytoplankton categories present in daily samples. The Shannon–Wiener (H') and Simpson ($1-D$) indices were selected based on their utility in marine ecology studies on large community samples [51,52]. Pielou’s evenness (J') is a measure of the cell density of each category relative to the overall population. The Shannon–Wiener index typically ranges between 1.5 and 3.5 while the Simpson index and Pielou’s evenness index ranges from 0 to 1.

2.6. Statistical Analysis

Results are presented as averages or medians plus/minus standard deviations. In the R coding language in the Rstudio program, statistical analyses were performed using the packages `vegan`, `BiodiversityR`, `tidyverse`, in the `ggplot2` format for data visualization [53,54]. `Decostand` and `dplyr` were used in the statistical analysis to test for normality and standardization. `Ggsci`, `ggrepel`, and `ggforce` were used to edit the text and labels of the plots [55,56].

The relative abundance of the phytoplankton groups rather than total abundance was used to more easily determine trends in the community over time [57]. Relationships between environmental parameters and IFCB data were examined using redundancy analysis (RDA) according to [58]. RDA involves a two-step process; a multiple linear regression is applied to each category in a response matrix, our IFCB data, using variables from an explanatory matrix, our environmental parameter data, and a PCA fit onto this intermediate matrix to reduce dimensionality to two explanatory axes [59].

IFCB data (cells/mL) was normalized using the Hellinger transformation, a convex standardization that helps minimize effects of different total abundances of major taxonomic groups [60]. Environmental data were transformed ($\log x + 1$) and standardized to achieve as normalized distribution as possible, confirmed by the Shapiro–Wilk test of normality, with as little collinearity between variables as possible, confirmed by the Variance Inflation Factor. RDA summary information and permutation tests were used to determine explained variance and significance of the model, axes, and vectors. RDA figures include points for each higher taxonomic group, vectors for each environmental parameter, and points for each daily sample. In each RDA figure, ellipsoids were drawn around pre- and post-storm period points. These ellipsoids represent normalized 95% confidence intervals of community composition by multivariate t -distribution (p -value < 0.05).

To visualize the day-to-day data in bubble plots, we grouped categories into a single genus when there was more than one species classified (e.g., for *Chaetoceros* spp.). Abundance of taxa (cells ml^{-1}) was represented by the traits of bubbles (size and color)

and organized by major phytoplankton category: diatoms, chlorophytes, cyanobacteria, dinoflagellates, cryptophytes, euglenoids, and raphidophytes. The data are represented on an exponential scale to facilitate visualization, but no transformation was applied. When no bubble was displayed, abundance was equal to zero. Bubble plots were performed in R software v4.0.5 [53], and RStudio v2023.12.0 [55] using “ggplot2” v.3.5.0 [54] and “RColorBrewer” v.1.1-3 packages [56].

3. Results

There is a rich diversity of phytoplankton detected with the IFCB at this location, much of which is reflected in the >90 phytoplankton categories (Table S1). Unfortunately, we were not able to identify the significant population of phytoplankton that are <10 µm, but are aware that numerically, they are important contributors to the overall community. The most readily detectable taxa with the IFCB are the diatoms, which includes common coastal species such as *Thalassiosira* sp., *Asterionellopsis* sp., *Chaetoceros* spp., and *Coscinodiscus* sp. Further, there are a variety of marine cyanobacteria present year-round, but after large storm events, freshwater species appear for a short time as a result of being flushed into the bay by the major rivers. Chlorophytes are also common, but few are difficult to distinguish between species unless they have very distinctive features (Table S1).

3.1. 2016 Tax Day Flood

Water temperatures increased from pre-storm values of 20.78 ± 1.49 °C to 24.07 ± 0.82 °C post-storm (Table 2); the shift was consistent with normal seasonal temperature trends rather than because of the storm event. Salinity pre-storm (16.99 ± 3.72) was higher than post-storm (12.61 ± 2.87), indicating that flood waters had influenced the sampling site. Precipitation pre-storm (6.68 cm) was half that which fell after the storm (>12 cm) (Table 2). There was an overall (total) increase in chl-a post-storm (10.30 ± 4.09 µg/L) compared with pre-storm values (7.91 ± 1.13 µg/L), with maximum values of 15.13 µg/L recorded (Table 2).

Table 2. Environmental data collected at the sampling site. Minimum (min), maximum (max), and average values (plus or minus standard errors) were calculated for temperature (°C), salinity, and chlorophyll-a (µg/L), while total precipitation (ppt, cm) and the highest daily total precipitation are reported (max value) for rainfall. Study periods are defined in Table 1. Refer to [38] for additional environmental data pre- and post-storms.

	Overall Average ± SE	Pre-Min	Pre-Max	Pre-Average ± SE	Post-Min	Post-Max	Post-Average ± SE
2016 Tax Day Flood							
Temp	22.48 ± 2.03	17.83	22.51	20.78 ± 1.49	22.57	25.38	24.07 ± 0.82
Sal	14.73 ± 3.97	10.96	23.42	16.99 ± 3.72	9.56	20.16	12.61 ± 2.87
Ppt	18.73 (total)	0	6.6	6.68 (total)	0	3.53	12.05 (total)
Chl- <i>a</i>	9.14 ± 3.27	5.69	9.84	7.91 ± 1.13	3.34	15.13	10.30 ± 4.09
2017 Hurricane Harvey							
Temp	28.83 ± 1.74	24.22	31.37	29.93 ± 1.33	25.02	29.53	27.69 ± 1.33
Sal	20.83 ± 2.25	7.32	31.85	26.88 ± 4.64	4.50	21.00	14.52 ± 5.56
Ppt	67.75 (total)	0	4.54	9.74 (total)	0	21.94	58.01 (total)
Chl- <i>a</i>	8.65 ± 2.46	3.47	13.75	10.14 ± 2.30	3.92	8.95	7.09 ± 1.46
2019 Tropical Storm Imelda							
Temp	28.20 ± 2.28	23.40	30.88	29.22 ± 2.39	23.95	28.65	27.09 ± 1.51
Sal	21.13 ± 4.92	21.60	28.00	25.55 ± 1.68	13.81	20.29	16.33 ± 1.79
Ppt	45.38 (total)	0	0.10	0.18 (total)	0	17.29	45.20 (total)
Chl- <i>a</i>	7.42 ± 8.78	3.03	6.88	4.36 ± 1.09	1.81	10.36	6.20 ± 2.71
2021 Winter Storm Uri							
Temp	13.63 ± 1.74	10.65	15.55	13.92 ± 1.48	9.19	15.47	13.33 ± 1.93
Sal	23.61 ± 1.41	19.84	26.33	23.44 ± 1.68	22.31	25.64	23.78 ± 1.03
Ppt	2.77 (total)	0	1.72	2.22 (total)	0	0.43	0.55 (total)
Chl- <i>a</i>	4.47 ± 1.29	2.68	7.06	4.28 ± 1.38	1.85	5.89	4.68 ± 1.14

In Spring 2016, prior to the flood, the abundance of diatoms relative to other groups was greatest, accounting for ~52% of the community (range from minimum to maximum: 22–71%), while in the post flood period examined, the relative abundance decreased to an average of 37% but the ranges were similar (18–77%) (Figure 2a). In general, the relative abundance of dinoflagellates (22%) did not change with the passage of the flood (6–58%), except when the storm was immediately over the sampling station. At this time, they accounted for up to 50% of the community. Chlorophytes and euglenoids were impacted by the flood event (Figure 2a). Pre-storm chlorophytes accounted for a smaller portion of the community (6–21%, average: 13%) than following the storm (9–35%, average: 22%). For euglenoids, there was a greater relative abundance after the storm (average: 5%) than prior (average: 2%). Cyanobacteria made up only 3% of the relative abundance of the community but could be up to 17% on some days. Similarly, cryptophytes were variable over the dates examined, usually accounting for 5 to 10% of the community, with an average of 9%, and varying from 0 to 31%. Raphidophytes accounted for the smallest fraction of the community (0.2%) and were only present on 11 of the 31 sampling days.

An RDA was used to examine the relationship between environmental parameters and the phytoplankton community during the 2016 storm study period (Figure 3a; Table 3). The model is globally significant ($F = 2.228$, $p = 0.016$) and explains 10.93% of the variance in the daily community data. Temperature and chl-*a* were the only significant environmental parameters in the model (temperature: $F = 2.738$, $p = 0.043$, chl-*a*: $F = 2.729$, $p = 0.040$) while salinity was not significant. Only the first model axis, RDA1, was significant ($F = 5.251$, $p = 0.014$) and accounted for 15.6% of the community and species variation while the second axis, RDA2, was not significant ($F = 0.983$, $p = 0.714$) and only accounted for 2.9% of the variation.

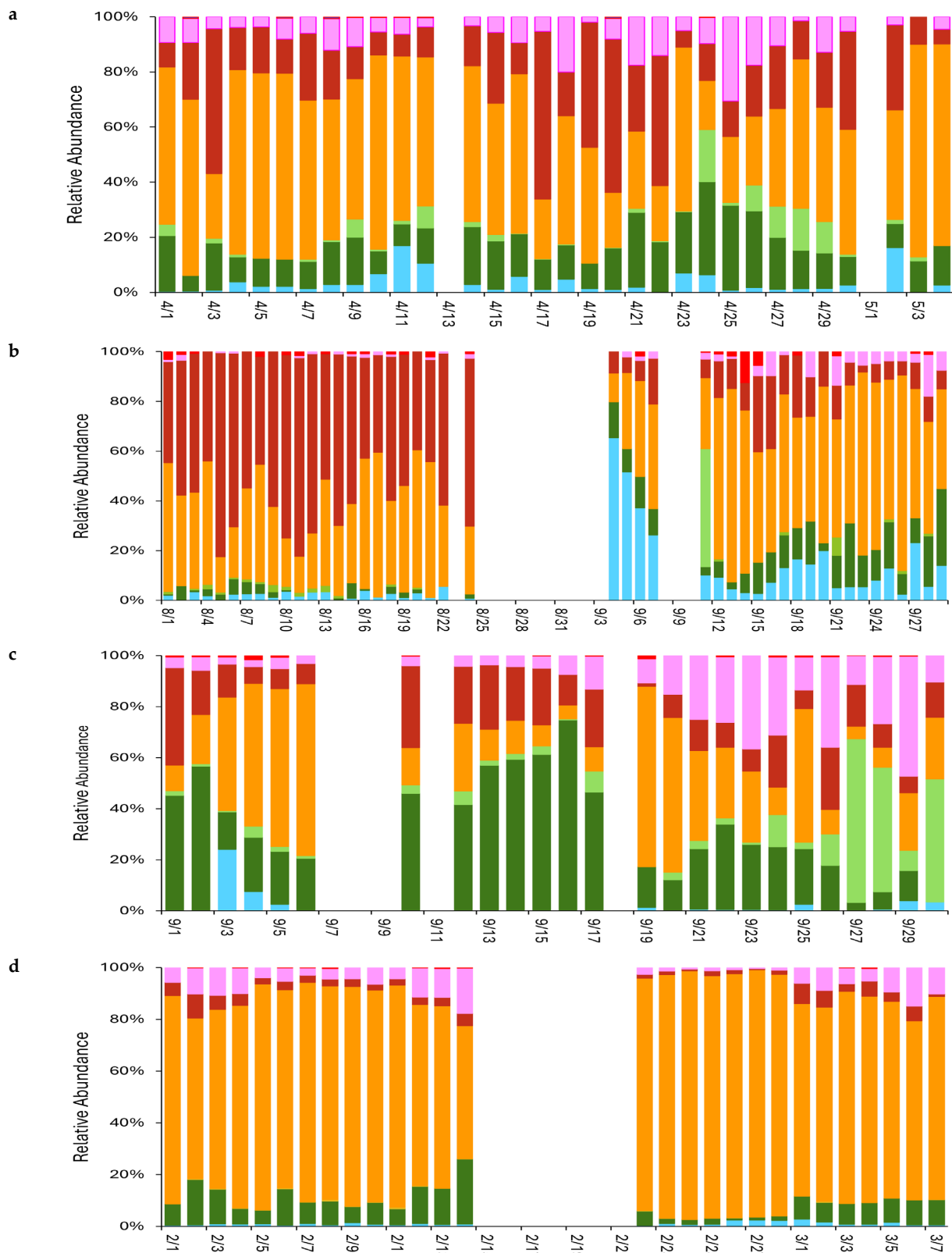


Figure 2. Relative abundances of the major taxonomic groups pre- and post-major storm events (denoted with a vertical dashed line). Phytoplankton were categorized as diatoms (orange), chlorophytes (dark green), cyanobacteria (blue), dinoflagellates (red), cryptophytes (pink), euglenoids (light green), and raphidophytes (light red) are shown. (a) Tax Day Flood in 2016, (b) Hurricane Harvey in 2017, (c) Tropical Storm Imelda in 2019, and (d) Winter Storm Uri in 2021.

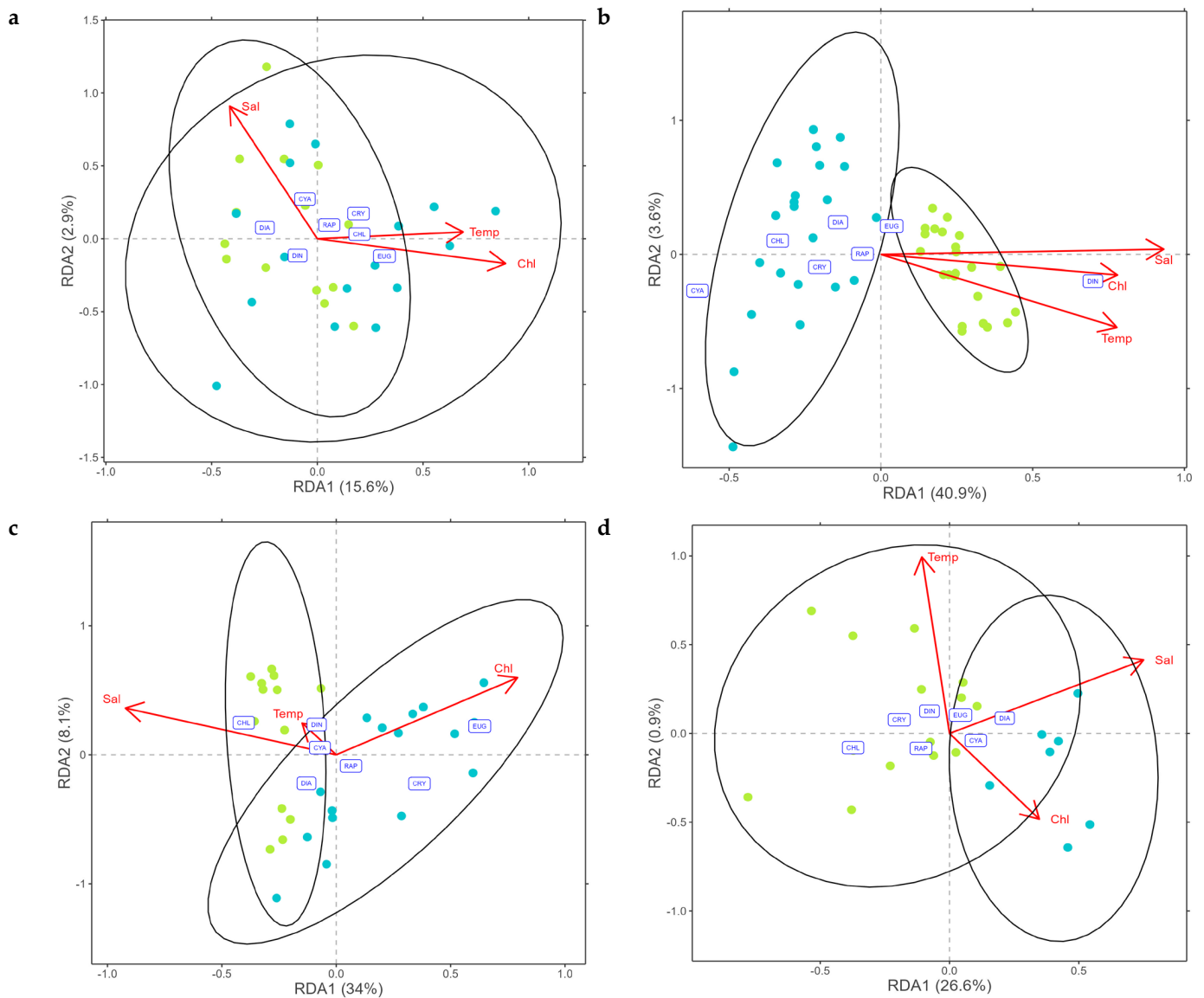


Figure 3. Redundancy analysis of the major taxonomic groups and significant water quality parameters pre- (green) and post- (blue) storm. Phytoplankton category codes: DIA—diatoms, CHL—chlorophytes, CYA—cyanobacteria, DIN—dinoflagellates, CRY—cryptophytes, EUG—euglenoids, and RAP—raphidophytes. Vector codes: Temp—temperature (°C), Sal—salinity, and Chl—chlorophyll-a (µg/L). (a) Tax Day Flood in 2016, (b) Hurricane Harvey in 2017, (c) Tropical Storm Imelda in 2019, and (d) Winter Storm Uri in 2021. These ellipsoids represent normalized 95% confidence intervals of community composition by multivariate t-distribution (p -value = 0.05).

Table 3. Summary information and significance values for RDA plots during each storm. Significance codes are: * = 0.05, ** = 0.01, *** = 0.001.

Model	Tax Day Flood	Hurricane Harvey Category 4	Tropical Storm Imelda	Winter Storm Uri
Year	2016	2017	2019	2021
Dates *	April 18	August 27–September 2	September 17–19	February 11–20

Table 3. Cont.

Model	Tax Day Flood	Hurricane Harvey Category 4	Tropical Storm Imelda	Winter Storm Uri
Constrained Variance	0.195	0.447	0.444	0.277
Residual Variance	0.802	0.553	0.557	0.723
Adjusted R-squared Value	0.109	0.407	0.377	0.149
Global sig.	0.016 *	0.001 ***	0.001 ***	0.096
Axis sig. RDA1	0.014 *	0.001 ***	0.001 ***	0.128
Axis sig. RDA2	0.714	0.085	0.045 *	0.964
Term sig. Temp	0.043 *	0.001 ***	0.205	0.682
Term sig. Sal	0.306	0.001 ***	0.001 ***	0.04 *
Term sig. Chl	0.04 *	0.016 *	0.005 **	0.176
VIF Temp	1.058	1.762	1.084	1.189
VIF Sal	1.175	1.764	1.275	1.088
VIF Chl	1.188	1.174	1.192	1.200

The pre-storm 95% confidence interval ellipsoid is almost completely enclosed within the post-storm ellipsoid, indicating that the phytoplankton community did not significantly change following the storm event. The larger size of the post-storm ellipsoid is consistent with the increase in diversity in the post-storm period (Figure 3). Higher chl-a and temperature values were more associated with the post-storm period while higher salinity was more associated with the pre-storm period. While communities were not significantly different, chlorophytes, euglenoids, and cryptophytes were more associated with the post-storm community.

3.2. 2017 Hurricane Harvey

Temperatures preceding Hurricane Harvey (29.93 ± 1.33 °C) were warmer than those following the storm (27.69 ± 1.33 °C) (Table 2). Salinity was most dramatically impacted by Hurricane Harvey, with pre-storm averages (26.88 ± 4.64) significantly higher than those after the storm (14.52 ± 5.56). This shift in salinity was driven by precipitation, of which more than 74 cm fell during the study period (Tables 1 and 2), with over 58 cm falling in just four days (between 26–29 August). This was more than the typical three-month summer rainfall (46.89 ± 4.75 cm), and lowered salinities at the IFCB sampling site for several weeks after the storm (Table 1). The flood waters also resulted in lowered chl-a (7.09 ± 1.46 µg/L) after the storm relative to before the storm (10.14 ± 2.30 µg/L).

While some phytoplankton groups (diatoms, cyanobacteria, and chlorophytes) in the community increased after Hurricane Harvey during the summer of 2017, other groups decreased (Figure 2b). Preceding the hurricane, the relative abundance of diatoms was 32% (14–58%) while afterwards this increased to 51% (12–80%). Similarly with cyanobacteria, which only accounted for 2% (1.9–6%) of the community before the hurricane, they then were 15% (0–65%) of the relative abundance. Chlorophytes in the pre-storm period were either absent or made up a very small fraction of the community (average = 3%), whereas after the hurricane's passage, they contributed to 16% of the community (1–34%). Similarly, cryptophytes were a small fraction of the community, varying from an average of 0.6% before to 5% after. Two weeks after the hurricane's passage, their abundance increased to 5–10%. Euglenoids and raphidophytes were essentially absent pre- and post-hurricane, accounting for a max of 3% and 4.8% and 0.5% and 0.3%, respectively.

Interestingly, dinoflagellate relative abundance decreased from 61% pre-hurricane (39–82%) to 12% afterwards (3–39%).

Relationships between environmental parameters and the phytoplankton community of Galveston Bay over the Hurricane Harvey study period were explored using RDA (Figure 3b; Table 3). The model is globally significant ($F = 11.31$, $p = 0.001$) and explains 40.74% of the variance in the daily community data. All three environmental parameters were significant (temperature: $F = 19.59$, $p = 0.001$; salinity: $F = 10.11$, $p = 0.001$; chl-a: $F = 4.24$, $p = 0.016$) with salinity most strongly driving the variation in daily community data. Only the first model axis RDA1 was significant ($F = 31.05$, $p = 0.001$) and accounted for 40.9% of the daily community and species variation while RDA2 ($F = 2.72$, $p = 0.085$) was not significant and only accounted for 3.6%.

The ellipsoids representing normalized 95% confidence intervals around pre-storm points and post-storm points were separated with very little overlap, indicating the post-storm community significantly deviated from pre-storm conditions. The post-storm group had a larger range, larger ellipsoid, and more outliers than the pre-storm group, representing a more diverse community in the period following Hurricane Harvey. Pre-storm points were correlated with higher temperature, salinity, and chl-a values while post-storm points were correlated with lower values. Dinoflagellates were strongly associated with the pre-storm community while chlorophytes and cyanobacteria were strongly associated with the post-storm community. Euglenoids, diatoms, and cryptophytes were associated more with the post-storm community than pre-storm and were the groups which occupied the most points in common.

3.3. 2019 Tropical Storm Imelda

Water temperatures after Tropical Storm Imelda decreased, with pre-storm temperatures (29.22 ± 2.39 °C) higher than post-storm (27.09 ± 1.51 °C) (Table 2). This change was driven by seasonal fluctuations rather than the storm. Changes in salinity were however driven by the storm, with a drop from 25.55 ± 1.68 to 16.33 ± 1.79 . A substantial amount of precipitation fell during the storm (44.35 cm), with less thereafter (Table 2). Values for chl-a preceding the storm varied from 3 to 7 µg/L, while after the storm they were ~2 µg/L for a few days before increasing to between 6–10 µg/L (Table 2).

Unlike with the previous storm events, diatoms made up a relatively small proportion of the phytoplankton community prior to (18%; 5–67%) and immediately after (20%; 5–82%) the storm (Figure 2c). Dinoflagellates were also similar pre- and post-storm, although more variable, with an average of 21% (7–38%) and 17% (1–47%), respectively. Cyanobacteria on the other hand, were largely absent, often less than 4%, but closer to 1%. Chlorophytes made up a larger proportion of the community (50%) pre-storm (15–75%), but this was greatly diminished after the storm to 13% (0–35%). In the weeks after Tropical Storm Imelda, cryptophytes became proportionally more dominant increasing from an average of 6% (3–13%) to 20% (3–47%). A week after the storm had passed, a euglenoid bloom was observed, with this group averaging around 3% (0.4–8%) to as much as 64% (average of 29%). Thereafter, the euglenoids rarely accounted for more than 5% of the community. Raphidophytes made up the lowest proportions of the phytoplankton community (0.3%) pre- and post-storm.

An RDA was used to examine the relationship between environmental parameters and the phytoplankton community during the Tropical Storm Imelda study period (Figure 3c; Table 3). The model is globally significant ($F = 6.64$, $p = 0.001$) and explains 37.67% of the variance in the daily community data. Salinity ($F = 13.59$, $p = 0.001$) and chl-a ($F = 4.84$, $p = 0.005$) were significant environmental parameters in the model and both strongly drove the community variation. Temperature ($F = 1.49$, $p = 0.205$) was non-significant and drove community variation the least. Both the first and second axis models, RDA1 ($F = 15.27$, $p = 0.001$) and RDA2 ($F = 3.63$, $p = 0.045$), were significant and accounted for 34% and 8.1% of the community and species variation, respectively.

The pre- and post-storm 95% confidence interval ellipsoids are partially separated but somewhat overlap, not indicating a significant shift in the phytoplankton community following the storm event. The larger size and width of the post-storm ellipsoid is associated with an increase in diversity following the storm event. Pre-storm points were correlated with higher temperature and salinity values while post-storm points were correlated with higher chl-a values. Chlorophytes were strongly associated with pre-storm points while euglenoids and cryptophytes were strongly associated with post-storm points. Cyanobacteria, diatoms, and dinoflagellates were not particularly associated with either study period, diatoms, and raphidophytes were not particularly associated with either study period.

3.4. 2021 Winter Storm Uri

Water temperatures before the 2021 Texas Freeze began near 15 °C and dropped to around 10 °C and stayed very low for ten days (Table 2). These were lower temperatures than the previously recorded low in the area which occurred in 1909 [61]. The first Winter Weather Advisory in Galveston was issued on February 11th and the temperatures continued to drop until February 16th. These record-breaking low air temperatures were associated with a La Niña winter super-cold wave event. The temperature steadily increased until the morning of February 20 when the winter storm passed. Salinities, precipitation, and chl-a did not vary pre- and post-storm (Table 2).

In the winter, diatoms (84%) accounted for most of the phytoplankton community at the sampling location (Figure 2d), with little variability pre- (51–87%; average=76%) and post- (66–96%; average=87%) freeze. Dinoflagellate and cyanobacteria proportions were relatively stable during the Texas Freeze study period, varying from 2% to 14% with an average of only 4% and from 0.4% to 3% with an average of 0.8%, respectively. Chlorophytes and cryptophytes essentially disappeared immediately after the storm, before returning to winter levels. Chlorophytes typically varied from 5 to 25%, while cryptophytes varied from 3 to 15% and average of ~6%. Euglenoids and raphidophytes were almost completely absent from the community (<0.1%).

An RDA was used to examine the relationship between environmental parameters and the phytoplankton community during the Texas Freeze study period (Figure 3d; Table 3). The model is globally significant ($F = 2.17, p = 0.096$) to $p = 0.1$ and explains 14.89% of the variance in the daily community data. Salinity was a significant environmental variable ($F = 4.35, p = 0.04$) in the model, along with chl-a ($F = 1.87, p = 0.176$) and temperature ($F = 0.28, p = 0.682$) being non-significant but with temperature and salinity mostly strongly driving the community and species variation. Neither of the model axes, RDA1 ($F = 6.25, p = 0.128$) accounting for 26.6% of the community and species variation, and RDA2 ($F = 0.21, p = 0.964$) accounting for 0.9% of the variation were significant.

Pre- and post-storm ellipsoids, representing normalized 95% confidence intervals around points in each period, were partially overlapping, indicating the community did not significantly shift following the storm event. The post-storm ellipsoid is similar in size to the pre-storm ellipsoid, indicating the community diversity did not significantly increase following the storm event. Post-storm points were correlated with changes in salinity and chl-a values while pre-storm points were correlated more with changing temperature. No phytoplankton group was significantly more associated with either period while chlorophytes and cryptophytes were more present in the pre-storm period and diatoms were more present in the post-storm period.

3.5. Ecological Diversity

Storm events caused varying effects on the diversity of the phytoplankton community in Galveston Bay. The pre-storm species richness was driven by season, with median values in summer < spring/fall < winter (Figure 4a). The weaker wet storms in 2016 (also 2015 and 2018 in 38), along with the cold wave in 2021, had lower species richness post-storm while the stronger storms Hurricane Harvey in 2017 and Tropical Storm Imelda in 2019,

which involved more localized precipitation at our sampling station, had similar median richness pre- and post-storm (Figure 4a).

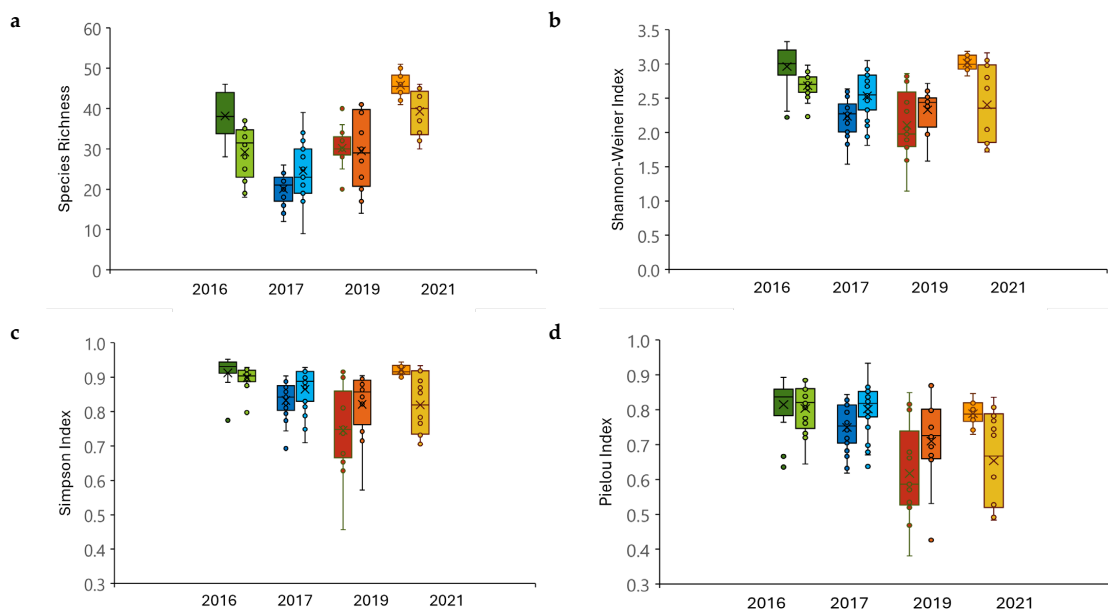


Figure 4. Diversity indices calculated for the phytoplankton community pre- (left) and post- (right) major storm events: Tax Day Flood in 2016 (green), Hurricane Harvey in 2017 (blue), Tropical Storm Imelda in 2019 (red), and Winter Storm Uri in 2021 (orange). (a) Species richness, (b) Shannon–Weiner index, (c) Simpson index, and (d) Pielou index.

In general, the Galveston Bay phytoplankton communities had greater diversity prior to the 2016 and 2021 storms, and less so in 2017 and 2019, based on the Shannon–Weiner index which had median values of >3 and <2.3 , respectively (Figure 4b). The median Shannon–Weiner index was lower after the 2016 and 2021 storms, dropping to 2.7 and 2.3 respectively. On the other hand, the median values increased to >2.4 after 2017 and 2021 storms, respectively. The range (based on the box plot percentiles) was greatest after the 2021 super-cold wave event, but least after the 2016 flood event, reflecting that these events had very different effects on the phytoplankton communities. Simpson’s index (1-D) median values varied between 0.75 (post-storm 2019) and 0.93 (pre-storm 2016) (Figure 4c), with shifts to higher and lower diversity mirroring the patterns observed for the Shannon–Weiner index (Figure 4b).

In 2016 and 2017 (pre- and post-storm), median Pielou index values were high and similar (0.84 and 0.82, and 0.75 and 0.82, respectively), indicating that all categories (genera) are represented in similar numbers in the daily samples (Figure 4d). By contrast, the median Pielou index was lower (0.58) before Tropical Storm Imelda in 2019 than post-storm (0.73) while the opposite was observed in 2021, with the Pielou’s index at 0.79 before the storm but 0.67 afterwards (Figure 4d). In addition, the range of Pielou values was broader during the 2019 and 2021 sampling periods, indicating that one or few categories were dominating the daily samples.

3.6. Dominant Phytoplankton Shifts

In 2016, the diatoms *Asterionellopsis* sp., *Chaetoceros* spp., *Ditylum* sp., *Entomoneis* spp., *Leptocylindrus* spp., and *Thalassiosira* spp., were present in significantly (4- to 10-fold) higher cell densities pre-storm than post-storm (Figure 5a). Similarly, the cyanobacteria *Anabaena* sp., the dinoflagellate *Karenia mikimotoi*, the cryptophyte *Cryptomonas* spp., and the euglenophyte *Eutreptiella* spp. were present in elevated cell densities pre-storm than post-storm (Figure 5a). Only the green algae *Pyramimonas* sp. were present in 3–4-fold higher cell densities post-storm relative to pre-storm conditions.

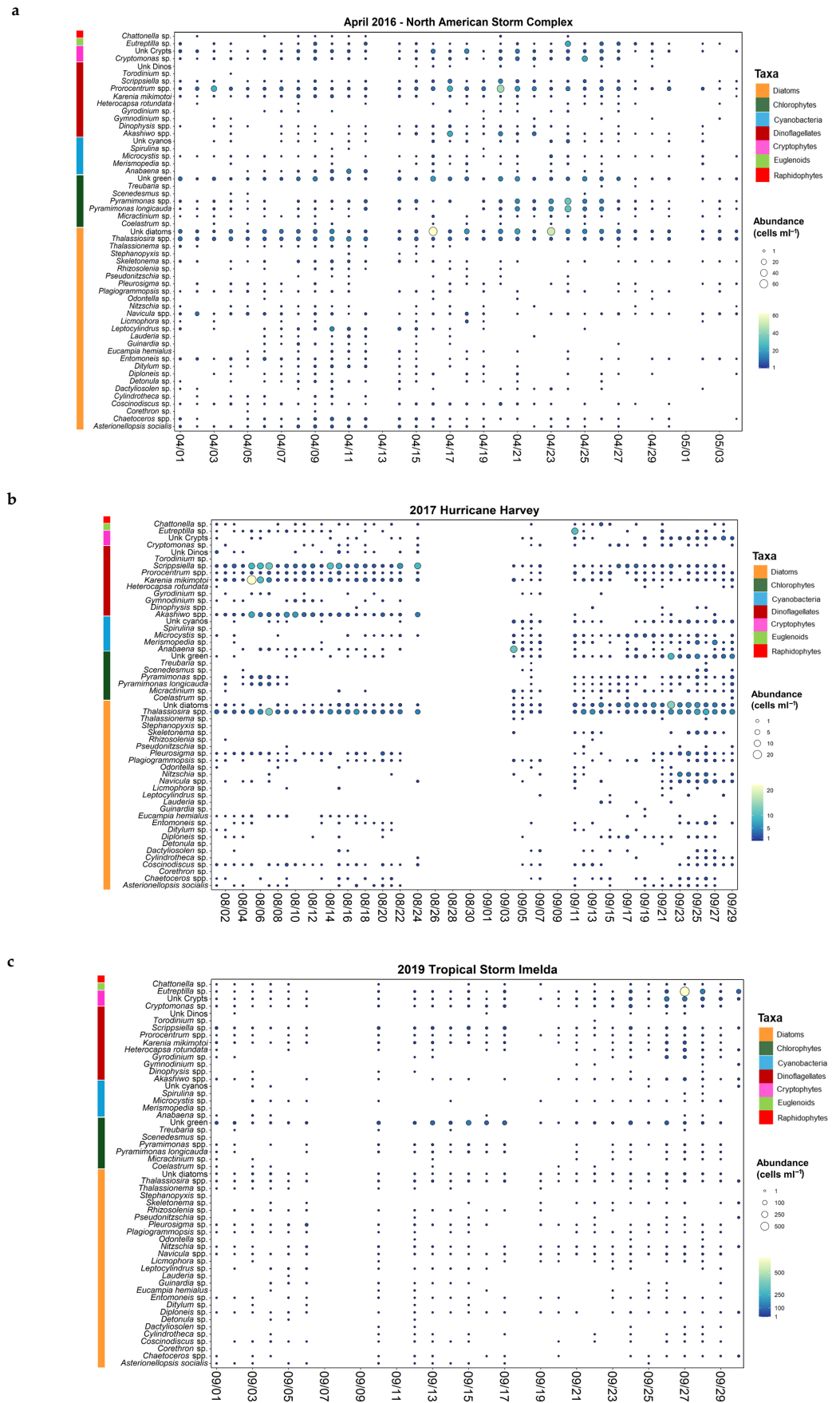


Figure 5. Cont.

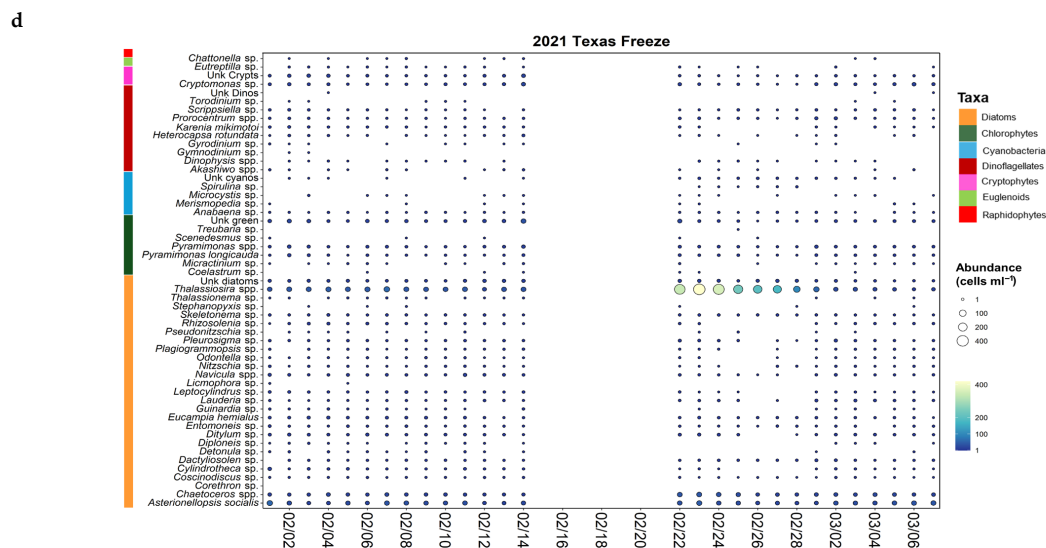


Figure 5. Bubble plots were used to examine changes in the abundance of the major phytoplankton categories classified with the IFCB pre- and post-major storm events (denoted with a vertical dashed line). (a) Tax Day Flood in 2016, (b) Hurricane Harvey in 2017, (c) Tropical Storm Imelda in 2019, and (d) Winter Storm Uri in 2021. Bubble size and the continuous color scale represent the abundance (cells mL⁻¹) (data no transformed). No bubble was displayed when the abundance was equal to zero. Data is shown as day to day (MM/DD) in the x-axis. A side color bar refers to each major phytoplankton category: diatoms (orange), chlorophytes (dark green), cyanobacteria (blue), dinoflagellates (red), cryptophytes (pink), euglenoids (light green), and raphidophytes (light red).

By contrast, cell densities of almost all species were lower prior to Hurricane Harvey in 2017 (Figure 5b). After the storm’s passage, the benthic diatoms *Navicula* spp., and *Nitzschia* spp., were present in 13 times higher cell densities. Given the wind driven resuspension of sediments because of the storm, this was not entirely surprising, but they may not have been captured without the daily sampling accomplished with the IFCB. Further, as a result of the flooding associated with this storm, numerous freshwater and other cyanobacteria were detected at the IFCB sampling station in high cell densities including species such as *Anabaena* sp., *Merismopedia* sp., *Microcystis* sp. which we were able to identify and others which were certainly cyanobacteria based on their cellular characteristics, but not as readily identifiable (Figure 5b). The euglenophyte *Eutreptiella* spp. and an unknown cryptophyte also were found to be in high cell densities (5- to 15-fold) post-storm compared to pre-storm.

In 2019, cell densities pre- and post-storm either doubled or halved (Figure 5c). The only exceptions were the dinoflagellates *Akashiwo sanguinea*, *Gyrodinium* sp., and *Heterocapsa* sp., which appeared to be 12- to 40-times higher in cell densities than post-storm compared to before the storm. These are all known harmful algal bloom species. Again, we found the euglenophyte *Eutreptiella* spp. and an unknown cryptophyte also were found to be in high cell densities (5- to 15-fold) post-storm compared to pre-storm.

In 2021, we generally found much higher overall cell densities of all species, but especially the diatoms (Figure 5d compared with Figure 5a–c), perhaps given that this sampling effort was focused during the winter. Most categories had similar cell densities before and after the storm. The most notable change was the significant increase in *Thalassiosira* spp. after the storm relative to those present before the storm (Figure 5d).

4. Discussion

The extreme weather patterns that occur in subtropical areas play a pronounced role in hydrogeological processes that influence phytoplankton communities in estuarine systems [3,9,14]. The IFCB monitoring made it possible to detect species of euglenophytes and cryptophytes in this study which are known to play important roles in food web dynamics but are often overlooked by traditional approaches [62,63]. Dinoflagellates, in-

cluding those known to cause red tide blooms and/or harmful bloom events, are commonly present, but rarely at densities which would cause concern at this location. In the middle, western, and eastern sectors of the bay and in the bayous (Figure 1), dinoflagellates and other harmful algal bloom species have been documented to occur at elevated cell densities, leading to hatchery closures and/or fish kill events [7,63,64]. Given that climate conditions are projected to become more unstable, pulse disturbances leading to phytoplankton community shifts due to alterations in temperature, light availability, and nutrient supply of varying magnitude and duration will be seen more frequently [3,13,65–67]. Prior studies suggest that, in addition to short term direct precipitation, increased freshwater inflow and its effects on nutrient and light levels can have a larger impact on long term phytoplankton community structure in many estuaries [68,69]. Further, if an ecosystem is experiencing eutrophication prior to, or because of the pulse disturbance, this will increase the absolute scale of the chl-a response [18]. Indeed, earlier studies in Galveston Bay have emphasized the influence that freshwater inflows, and associated nutrients and hydrography, have in shaping phytoplankton communities (e.g., [4,7,8,44]). The sampling locations in these studies were within the main water body of the bay and often closer to riverine inputs, while in the present study, the IFCB is located adjacent to the Gulf of Mexico, some ~50 km from the major freshwater sources. While these historical studies are key for understanding the “estuarine or bay” phytoplankton population composition and dynamics, the current study findings may not always align because of the difference in sampling location, and hence, factors influencing the community.

Diatoms make up the largest fraction of the Galveston Bay phytoplankton community in the colder and more saline conditions, particularly in cooler months ([7,38], present study); this has also been observed in other sub-tropical estuarine systems [70]. Winters had lower relative abundances of other major phytoplankton, particularly euglenoids and cryptophytes [38]. Summers, on the other hand, had higher proportions of these groups, as well as dinoflagellates. This cycle of seasonally alternating diatom and dinoflagellate abundance is consistent with published studies assessing community structure using other methods (e.g., [4,8,71]). While winter and summer phytoplankton communities and environmental conditions are relatively stable, fall and spring are periods of greater variability. Changing environmental parameters (e.g., temperature, salinity) in these transitional seasons (i.e., autumn/fall and spring) have been known to affect phytoplankton community dynamics and bloom formation [72,73]. Roelke et al. [44] and Dorado et al. [8] found that many non-linear-related processes such as nutrient flux, turbidity, water column mixing, and freshwater inflow drive community changes within Galveston Bay. Along with these processes, saltwater intrusion can strongly influence estuarine phytoplankton communities by transporting resuspended sediment and nutrient rich water, altering light and nutrient availability [74]. This is of particular importance to this study given the proximity of the sampling location to the Gulf of Mexico.

This study examined four major storm events which had differing effects on the phytoplankton community. While these storm events are known to have differed in the volume and duration of localized rainfall (Table 1) and wind, there was also a variety of environmental processes which ultimately altered community structure. Stelzer et al. [18] proposed that differing intensities of pulse disturbance events affect not only the impact but also the longevity of the effects to phytoplankton communities. The 2016 storm event had non-significant changes in the phytoplankton community (see overlapping ellipsoids in the RDA model and similar communities) (Figures 3a and 5a). This storm had the least significant RDA model that explained the lowest proportions of variance of any of the storm models (Table 3). The 2018 storm event (Independence Day Flooding) had more than twice the precipitation of the 2016 storm and a stronger shift in the community composition was recorded following the storm [38]. The phytoplankton responses to these events were similar those observed for Hurricanes Dennis and Floyd in 1999 which impacted North Carolina’s Pamlico Sound, with fast growing, opportunistic taxonomic groups such as

chlorophytes and cryptophytes increasing, while the larger, slow-growing dinoflagellates decreased in abundance [3].

More impactful storms with greater precipitation and larger changes to environmental parameters are likely to have stronger influences on the phytoplankton community [13]. Freshwater inflows (river discharge) from flooding, bringing with it changes in nutrient levels and turbidity, have the potential to affect phytoplankton communities on a larger scale and over a longer period than only precipitation caused changes in salinity [9]. However, both flooding and direct precipitation can have multiplicative impacts on community change depending on their proximity and severity [14]. The tropical storm systems in 2017 and 2019, Hurricane Harvey and Tropical Storm Imelda, had much higher localized precipitation over the sampling site, nearly three times more than the 2018 storm. Because of the rainfall, Hurricane Harvey caused floodwaters from the Trinity and San Jacinto Rivers to transport high volumes of cool, fresh, sediment- and nutrient-rich water into Galveston Bay [39], which were flushed past the sampling site (Figure 1) [27]. These storms (Hurricane Harvey and Tropical Storm Imelda) had a larger impact on the phytoplankton community (Figure 3), with the RDA model ellipsoids being either completely or mostly separate (Figure 3b,c), indicating that there was a 95% confidence that the communities were different. These findings are also supported by significant models explaining much of the community variation (Table 3). After Hurricane Harvey, there was a notable decline in chl-a as the biomass was initially flushed out of the bay [75], with a concurrent shift in the community [27]. There was a massive influx of freshwater (3–5 times the volume of the bay; [76]) and with it, associated cyanobacteria accounting for a larger proportion of the community. Tropical Storm Imelda resulted in an increase in chl-a and a community shift similar to that observed with the 2016 storm, and an increased proportion of chlorophytes, euglenoids, and cryptophytes (Figure 2). In addition to these distinctions, Harvey caused a change in the community that persisted for over two months while the Imelda community returned to pre-storm community composition about a month after the storm event (Figures 2 and 3). Studies vary but most agree that it took approximately three months for all the freshwater from Harvey to be discharged from the Bay [61,76]. On the other hand, it took a relatively short time for Imelda to be completely flushed (weeks; present study). Wetz and Paerl [14] observed notably distinct ecological effects following storms of different strengths; they associated these changes to variable nutrient influx and water column mixing. These factors were likely contributors to the larger storm in their study coinciding with a decrease in algal biomass, similar to observations for Hurricane Harvey. The increased inflow of nutrient and sediment rich waters during Harvey and the extent of the subsequent flooding [27,75], compared to shorter Imelda flooding, likely was the forcing factor of the extended duration of the community shift observed in Galveston Bay.

The 2021 Texas Freeze was the only major storm event examined herein associated with a super-cold wave (the 2020/2021 La Niña winter); this had a noticeably different effect on the phytoplankton community. Diatoms, already present in high proportions for the winter, accounted for almost 100% of the community for several days following the cold wave (Figures 2d and 5d). Ding et al. [17] and references therein reported smaller phytoplankton species are associated with colder temperatures. This has led to the miniaturization of phytoplankton in many estuaries including the Pearl River Estuary in the South China Sea (see [17]). The RDA model did not show a significant change in the community (Figure 3d). Different types of pulse disturbances are known to have differing effects on communities, particularly disturbances that are uncommon for an ecosystem [13]. Hence, while the shift to more diatoms and fewer other taxa was unexpected, perhaps it is more related to the unusual nature of freezes in a subtropical estuary. These observations are critical though, particularly as with climate change driven changes, more freezes may occur in subtropical estuaries just as more severe (strength, duration, frequency) storms are predicted [77,78]. These changes to storm events are also likely to increase the impact that they have on phytoplankton communities with ecosystem-wide implications.

Community Shifts

As with previous studies in Galveston Bay and other estuaries, we found that diversity was variable between years, seasons, and storms (Figure 4), with values between 2.2 and 3.3 for the Shannon–Weiner diversity index, similar to those reported by Huang et al. [68] and Pinckney et al. [4]. In addition, as with other estuarine studies, we also report that storm events cause a decrease [16] and increase [79] in community diversity. These shifts in cell diversity were found to be storm-dependent and likely due to shifts in the levels of particulate matter and nutrient concentrations associated with storms.

Unlike previous studies in Galveston Bay that examined phytoplankton communities throughout the entire bay system, we did not observe higher diversity in summer and fall (e.g., [4,7]), in fact the opposite was observed. This is because primary productivity within the bay is driven by nutrient (as nitrogen) pulsing events associated with riverine inputs, while our sampling site for these studies was adjacent to the Gulf of Mexico, some 50 km away from the major rivers that deliver nutrients into the bay.

In 2019, freshwater discharges associated with the storm triggered increases in dinoflagellates and other flagellates (euglenophytes and cryptophytes) relative to other groups (Figures 2–4), like that observed by Anglès et al. [15] for other Texas estuaries impacted by storms. However, this was not the case after the 2016 and 2017 storms which likely did not produce sufficient discharge to influence phytoplankton at the sampling station and significant discharge respectively that resulted in hydrologic displacement of the phytoplankton community (Figures 2–4).

5. Conclusions

Phytoplankton community studies utilizing automated IFCB image classification allow for a deeper understanding of storm impacts than many other established methods (Table S2). Until now, there are no analyses of multiple pulse disturbance events using an IFCB. The strength of the IFCB as a community analysis tool is that it can be used to examine species or genera level dynamics on a finer scale and over a longer time frame, as well as pulse disturbance events. The results of this study complement other examinations of extreme events which have found that relatively small tropical storms and hurricanes (herein the 2016 Tax Day Flood and 2019 Tropical Storm Imelda) can lead to significant increases in phytoplankton biomass (e.g., [14]), whilst large storms will flush phytoplankton out of estuaries (herein 2017 Hurricane Harvey) [27,75]. Collectively, these studies reveal that the phytoplankton response depends on both the characteristics of the storm and the physical–chemical conditions of the estuary before its passage (Table S2) [18]. The major limitation of the present study is that we had only one sampling station. This means we may have missed any “hot spots” for trophic transfer and/or biogeochemical dynamics as reported elsewhere (e.g., [14]). However, the daily sampling in this one location provided a deeper understanding of how the community structure was being altered by each of these storms. Ongoing studies are needed to capture both features and details to fully understand the impact of perturbations from extreme weather events on estuarine ecosystems.

Supplementary Materials: The following supporting information can be downloaded at: <https://www.mdpi.com/article/10.3390/environments11100218/s1>, Table S1: Class list used in Random Forest classifier, separated by higher taxonomic group with information about distribution and formation; Table S2: Summary of the phytoplankton response which was dependent on both the characteristics of the storm and the physical–chemical conditions of the estuary before its passage, and afterwards.

Author Contributions: N.C. ran samples, performed the IFCB analysis, and performed the statistical analyses as part of his Master’s dissertation. J.L.S. established the IFCB protocols and classifier, identified the phytoplankton, ran samples, and QA/QC’d the data over 7 years. D.H. provided advice on IFCB operations and data interpretation, aided the statistical analyses and interpretation. A.Q. funded the work, interpreted the findings, and wrote the manuscript. All authors have read and agreed to the published version of the manuscript.

Funding: The IFCB was purchased with the support of Lance Robinson (retired) and two State Wildlife Grants (Federal Aid Grant No. 428577 and 475858) administered by Texas Parks and Wildlife Division. Subsequent research was made possible with funding from the Coastal Management Program administered by the Texas General Land Office (Grant Cycle #19), a grant funded by the Coastal Coordination Council by a cooperative agreement from the National Oceanic and Atmospheric Administration Award No. NA15-043-000-8388, and U.S. Fish and Wildlife Service Grant TX T-204-R-1 (F19AF01053).

Data Availability Statement: The data presented in this study are available on request from the corresponding author due to the embargo on Noah Claflin (MS student, first author) master's thesis. The original data presented in the study will be made openly available in a repository once the embargo is lifted.

Acknowledgments: We thank Heidi M. Sosik, Robert J. Olson for guidance and help with initial instrument set up and running. This work would not have been possible without the unending support from Yuki A. Honjo and McLane engineers, (Matthew Bach, Ivory Engstrom, Tom Fougere) who have provided assistance with IFCB operations and repairs and the countless undergraduates and graduate students who have collected samples over the years and helped build the classifier, especially Hannah Preischel Lee and Amelia McAmis. We thank Aurora Gaona Hernandez at Texas A & M University at Galveston for preparing the bubble plots for this manuscript. We also thank the three anonymous reviewers whose comments and suggestions greatly improved the final manuscript.

Conflicts of Interest: The authors declare no conflicts of interest.

References

1. Cloern, J.E.; Foster, S.Q.; Kleckner, A.E. Phytoplankton primary production in the world's estuarine-coastal ecosystems. *Biogeosciences* **2014**, *11*, 2477–2501. [[CrossRef](#)]
2. Hopkinson, C.S.; Smith, E.M. Estuarine respiration: An overview of benthic, pelagic, and whole system respiration. In *Respiration in Aquatic Ecosystems*; del Giorgio, P., Williams, P., Eds.; Oxford University Press: New York, NY, USA, 2005; pp. 122–146.
3. Paerl, H.W.; Valdes, L.M.; Peierls, B.L.; Adolf, J.E.; Harding, L.W. Anthropogenic and climatic influences on the eutrophication of large estuarine ecosystems. *Limnol. Oceanogr.* **2006**, *51*, 448–462. [[CrossRef](#)]
4. Pinckney, J.L.; Quigg, A.; Roelke, D.L. Interannual and seasonal patterns of estuarine phytoplankton diversity in Galveston Bay, Texas, USA. *Estuaries Coasts* **2017**, *40*, 310–316. [[CrossRef](#)]
5. Wells, M.L.; Karlson, B.; Wulff, A.; Kudela, R.; Trick, C.; Asnaghi, V.; Berdalet, E.; Cochlan, W.; Davidson, K.; De Rijcke, M.; et al. Future HAB science: Directions and challenges in a changing climate. *Harmful Algae* **2020**, *91*, 101632. [[CrossRef](#)] [[PubMed](#)]
6. Boynton, W.R.; Kemp, W.M.; Keefe, C.W. A comparative analysis of nutrients and other factors influencing estuarine phytoplankton production. In *Estuarine Comparisons*; Kennedy, V.S., Ed.; Academic Press: New York, NY, USA, 1982; pp. 69–90.
7. Örnólfsson, E.B.; Lumsden, S.E.; Pinckney, J.L. Nutrient pulsing as a regulator of phytoplankton abundance and community composition in Galveston Bay, Texas. *J. Exp. Mar. Biol. Ecol.* **2004**, *303*, 197–220. [[CrossRef](#)]
8. Dorado, S.; Booe, T.; Steichen, J.L.; McInnes, A.S.; Windham, R.; Shepard, A.; Lucchese, A.E.B.; Preischel, H.; Pinckney, J.L.; Davis, S.E.; et al. Towards an understanding of the interactions between freshwater inflows and phytoplankton communities in a subtropical estuary in the Gulf of Mexico. *PLoS ONE* **2015**, *10*, e0130931. [[CrossRef](#)]
9. Han, H.; Xiao, R.; Gao, G.; Yin, B.; Liang, S. Influence of a heavy rainfall event on nutrients and phytoplankton dynamics in a well-mixed semi-enclosed bay. *J. Hydrol.* **2023**, *617*, 128932. [[CrossRef](#)]
10. Bharathi, M.; Venkataramana, V.; Sarma, V. Phytoplankton community structure is governed by salinity gradient and nutrient composition in the tropical estuarine system. *Cont. Shelf Res.* **2022**, *234*, 104643. [[CrossRef](#)]
11. Luo, X.; Pan, K.; Wang, L.; Li, M.; Li, T.; Pang, B.; Kang, J.; Fu, J.; Lan, W. Anthropogenic inputs affect phytoplankton communities in a subtropical estuary. *Water* **2022**, *14*, 636. [[CrossRef](#)]
12. Wu, Y.; Guo, P.; Su, H.; Zhang, Y.; Deng, J.; Wang, M.; Sun, Y.; Li, Y.; Zhang, X. Seasonal and spatial variations in the phytoplankton community and their correlation with environmental factors in the Jinjiang River Estuary in Quanzhou, China. *Environ. Monit. Assess.* **2021**, *194*, 44. [[CrossRef](#)]
13. Jentsch, A.; White, P. A theory of pulse dynamics and disturbance in ecology. *Ecology* **2019**, *100*, e02734. [[CrossRef](#)] [[PubMed](#)]
14. Wetz, M.S.; Paerl, H.W. Estuarine phytoplankton responses to hurricanes and tropical storms with different characteristics (trajectory, rainfall, winds). *Estuaries Coasts* **2008**, *31*, 419–429. [[CrossRef](#)]
15. Anglès, S.; Jordi, A.; Campbell, L. Responses of the coastal phytoplankton community to tropical cyclones revealed by high-frequency imaging flow cytometry. *Limnol. Oceanogr.* **2015**, *60*, 1562–1576. [[CrossRef](#)]
16. Reyna, N.E.; Hardison, A.K.; Liu, Z. Influence of major storm events on the quantity and composition of particulate organic matter and the phytoplankton community in a subtropical estuary, Texas. *Front. Mar. Sci.* **2017**, *4*, 43. [[CrossRef](#)]
17. Ding, X.; Liu, J.; Liu, W.; Dai, S.; Ke, Z.; Guo, J.; Lai, Y.; Tan, Y. Phytoplankton communities miniaturization driven by extreme weather in subtropical estuary under climate changes. *Water Res.* **2023**, *245*, 120588. [[CrossRef](#)]

18. Stelzer, J.A.; Mesman, J.P.; Gsell, A.S.; de Senerpont Domis, L.N.; Visser, P.M.; Adrian, R.; Ibelings, B.W. Phytoplankton responses to repeated pulse perturbations imposed on a trend of increasing eutrophication. *Ecol. Evol.* **2022**, *12*, e8675. [[CrossRef](#)]
19. Copeland, B.J.; Bechtel, T.J. Species diversity and water quality in Galveston Bay, Texas. *Water Air Soil Pollut.* **1971**, *1*, 89–105. [[CrossRef](#)]
20. Alves-de-Souza, C.; González, M.T.; Iriarte, J.L. Functional groups in marine phytoplankton assemblages dominated by diatoms in fjords of southern Chile. *J. Plankton Res.* **2008**, *30*, 1233–1243. [[CrossRef](#)]
21. Ramond, P.; Siano, R.; Schmitt, S.; De Vargas, C.; Marié, L.; Memery, L.; Sourisseau, M. Phytoplankton taxonomic and functional diversity patterns across a coastal tidal front. *Sci. Rep.* **2021**, *11*, 2682. [[CrossRef](#)]
22. Sweet, J.A.; Bargu, S.; Morrison, W.L.; Parsons, M.; Pathare, M.G.; Roberts, B.J.; Soniat, T.M.; Stauffer, B.A. Phytoplankton dynamics in Louisiana estuaries: Building a baseline to understand current and future change. *Mar. Pollut. Bull.* **2022**, *175*, 113344. [[CrossRef](#)]
23. Edwards, K.F.; Thomas, M.K.; Klausmeier, C.A.; Litchman, E. Phytoplankton growth and the interaction of light and temperature: A synthesis at the species and community level. *Limnol. Oceanogr.* **2016**, *61*, 1232–1244. [[CrossRef](#)]
24. Badylak, S.; Philips, E.J. Spatial and temporal patterns of phytoplankton composition in a subtropical coastal lagoon, the Indian River Lagoon, Florida, USA. *J. Plankton Res.* **2004**, *26*, 1229–1247. [[CrossRef](#)]
25. Soares, M.C.S.; Lobão, L.M.; Vidal, L.O.; Noyma, N.P.; Barros, N.O.; Cardoso, S.J.; Roland, F. Light microscopy in aquatic ecology: Methods for plankton communities studies. *Methods Mol. Biol.* **2011**, *689*, 215–227. [[CrossRef](#)] [[PubMed](#)]
26. Álvarez, E.; Moyano, M.; López-Urrutia, Á.; Nogueira, E.; Scharek, R. Routine determination of plankton community composition and size structure: A comparison between FlowCAM and light microscopy. *J. Plankton Res.* **2014**, *36*, 170–184. [[CrossRef](#)]
27. Steichen, J.L.; Labonté, J.M.; Windham, R.; Hala, D.; Kaiser, K.; Setta, S.; Faulkner, P.C.; Bacosa, H.; Yan, G.; Kamalanathan, M.; et al. Microbial, physical, and chemical changes in Galveston Bay following an extreme flooding event, Hurricane Harvey. *Front. Mar. Sci.* **2020**, *7*, 186. [[CrossRef](#)]
28. Olson, R.J.; Sosik, H.M. A submersible imaging-in-flow instrument to analyze nano-and microplankton: Imaging flowcytobot. *Limnol. Oceanogr. Methods* **2007**, *5*, 195–203. [[CrossRef](#)]
29. Sosik, H.M.; Olson, R.J. Automated taxonomic classification of phytoplankton sampled with imaging-in-flow cytometry. *Limnol. Oceanogr. Methods* **2007**, *5*, 204–216. [[CrossRef](#)]
30. Veldhuis, M.J.W.; Kraay, G.W. Application of flow cytometry in marine phytoplankton research: Current applications and future perspectives. *Sci. Mar.* **2000**, *64*, 121–134. [[CrossRef](#)]
31. Sieracki, C.K.; Sieracki, M.E.; Yentsch, C.S. An imaging-in-flow system for automated analysis of marine microplankton. *Mar. Ecol. Prog. Ser.* **1998**, *168*, 285–296. [[CrossRef](#)]
32. Cunningham, A.; McKee, D.; Craig, S.; Tarran, G.; Widdicombe, C. Fine-scale variability in phytoplankton community structure and inherent optical properties measured from an autonomous underwater vehicle. *J. Mar. Syst.* **2003**, *43*, 51–59. [[CrossRef](#)]
33. Olson, R.J.; Shalapyonok, A.; Sosik, H.M. An automated submersible flow cytometer for analyzing pico-and nanophytoplankton: FlowCytobot. *Deep. Sea Res. Part I Oceanogr. Res. Pap.* **2003**, *50*, 301–315. [[CrossRef](#)]
34. Sosik, H.M.; Olson, R.J.; Neubert, M.G.; Shalapyonok, A.; Solow, A.R. Growth rates of coastal phytoplankton from time-series measurements with a submersible flow cytometer. *Limnol. Oceanogr.* **2003**, *48*, 1756–1765. [[CrossRef](#)]
35. Campbell, L.; Henrichs, D.W.; Olson, R.J.; Sosik, H.M. Continuous automated imaging-in-flow cytometry for detection and early warning of *Karenia brevis* blooms in the Gulf of Mexico. *Environ. Sci. Pollut. Res.* **2013**, *20*, 6896–6902. [[CrossRef](#)] [[PubMed](#)]
36. Henrichs, D.W.; Anglès, S.; Gaonkar, C.C.; Campbell, L. Application of a convolutional neural network to improve automated early warning of harmful algal blooms. *Environ. Sci. Pollut. Res.* **2021**, *28*, 28544–28555. [[CrossRef](#)] [[PubMed](#)]
37. Lee, H.A. Effects of Physical Disturbance on Phytoplankton Diversity and Community Composition in Galveston Bay, TX, during an Extreme Flooding Event. Master's Thesis, Texas A&M University, College Station, TX, USA, 2017; 78p.
38. Claflin, N. A Seven Year Analysis into the Phytoplankton Community of Galveston Bay Using IFCB Imagery. Master's Thesis, Texas A&M University, College Station, TX, USA, 2023; 125p.
39. Kiaghadi, A.; Rifai, H.S. Physical, chemical, and microbial quality of floodwaters in Houston following Hurricane Harvey. *Environ. Sci. Technol.* **2019**, *53*, 4832–4840. [[CrossRef](#)]
40. Schlegel, R.W.; Darmaraki, S.; Benthuisen, J.A.; Filbee-Dexter, K.; Oliver, E.C.J. Marine cold-spells. *Prog. Oceanogr.* **2021**, *198*, 102684. [[CrossRef](#)]
41. Wang, Y.X.; Kajtar, J.B.; Alexander, L.V.; Pilo, G.S.; Holbrook, N.J. Understanding the changing nature of marine cold-spells. *Geophys. Res. Lett.* **2022**, *49*, e2021GL097002. [[CrossRef](#)]
42. Gonzalez, L.A.; Lester, L.J. *State of the Bay: A Characterization of the Galveston Bay Ecosystem*, 3rd ed.; Texas Commission on Environmental Quality, Galveston Bay Estuary Program: Houston, TX, USA, 2011.
43. Lester, J.; Gonzalez, L.A.; Sage, T.; Gallaway, A. *The State of the Bay: A Characterization of the Galveston Bay Ecosystem*; Texas Commission on Environmental Quality, Galveston Bay Estuary Program: Houston, TX, USA, 2002.
44. Roelke, D.; Li, H.-P.; Hayden, N.; Miller, C.; Davis, S.; Quigg, A.; Buyukates, Y. Co-occurring and opposing freshwater inflow effects on phytoplankton biomass, productivity and community composition of Galveston Bay, USA. *Mar. Ecol. Prog. Ser.* **2013**, *477*, 61–76. [[CrossRef](#)]

45. Quigg, A.; Steichen, J.L.; Windham, R. *Galveston Bay: Changing Land Use Patterns and Nutrient Loading. Causal or Casual Relationship with Water Quality, Quantity, and Patterns?* Texas Commission on Environmental Quality and the U.S. Environmental Protection Agency: Houston, TX, USA, 2017.
46. Arar, E.J.; Collins, G.B. *Method 445.0: In Vitro Determination of Chlorophyll-a and Pheophytin a in Marine and Freshwater Algae by Fluorescence*; United States Environmental Protection Agency: Washington, DC, USA, 1997.
47. Tomas, C.R. *Identifying Marine Phytoplankton*; Elsevier: Amsterdam, The Netherlands, 1997.
48. Quigg, A.; McAmis, A.; Steichen, J.L.; Windham, R. *Phytoplankton Identification Guide for Texas Coastal Waters [Identification Guide]*; Texas A&M University at Galveston: Galveston, TX, USA, 2018.
49. Breiman, L. Random Forests. *Mach. Learn.* **2001**, *45*, 5–32. [[CrossRef](#)]
50. Krebs, C.J. *Ecological Methodology*; Harper and Row: New York, NY, USA, 1999.
51. Badsı, H.; Ali, H.O.; Loudiki, M.; Aamiri, A. Phytoplankton diversity and community composition along the salinity gradient of the Massa estuary. *Am. J. Hum. Ecol.* **2012**, *1*, 58–64. [[CrossRef](#)]
52. Interlandi, S.J.; Kilham, S.S. Limiting resources and the regulation of diversity in phytoplankton communities. *Ecology* **2001**, *82*, 1270–1282. [[CrossRef](#)]
53. R Core Team. *R: A Language and Environment for Statistical Computing*; R Foundation for Statistical Computing: Vienna, Austria, 2021. Available online: <https://www.R-project.org/> (accessed on 13 March 2023).
54. Wickham, H. *ggplot2: Elegant Graphics for Data Analysis*; Springer: New York, NY, USA, 2016. Available online: <https://ggplot2.tidyverse.org> (accessed on 13 March 2023).
55. Posit Team. *RStudio: Integrated Development Environment for R*; Posit Software, PBC: Boston, MA, USA, 2023. Available online: <http://www.posit.co/> (accessed on 13 March 2023).
56. Neuwirth, E. RColorBrewer: ColorBrewer Palettes V.1.1-3. 2022. Available online: <https://CRAN.R-project.org/package=RColorBrewer> (accessed on 13 March 2023).
57. Preston, F.W. The commonness, and rarity, of species. *Ecology* **1948**, *29*, 254–283. [[CrossRef](#)]
58. Borcard, D.; Gillet, F.; Legendre, P. *Numerical Ecology with R*; Springer: New York, NY, USA, 2011; Volume 2. [[CrossRef](#)]
59. Legendre, P.; Legendre, L. *Numerical Ecology*; Elsevier: Amsterdam, The Netherlands, 2012.
60. Legendre, P.; Gallagher, E.D. Ecologically meaningful transformations for ordination of species data. *Oecologia* **2001**, *129*, 271–280. [[CrossRef](#)]
61. NOAA. NOAA National Centers for Environmental Information Website. Available online: <http://ncei.noaa.gov> (accessed on 1 February 2023).
62. Valdes-Weaver, L.M.; Piehler, M.F.; Pinckney, J.L.; Howe, K.E.; Rossignol, K.; Paerl, H.W. Long-term temporal and spatial trends in phytoplankton biomass and class-level taxonomic composition in the hydrologically variable Neuse-Pamlico estuarine continuum, North Carolina, USA. *L&O* **2006**, *51*, 1410–1420. [[CrossRef](#)]
63. Thronson, A.; Quigg, A. Fifty five years of fish kills in Coastal Texas. *Estuaries Coasts* **2008**, *31*, 802–813. [[CrossRef](#)]
64. McInnes, A.; Quigg, A. Near-annual fish kills in small embayments: Casual versus causal factors. *J. Coast. Res.* **2010**, *26*, 957–966. [[CrossRef](#)]
65. Du, J.; Park, K.; Dellapenna, T.M.; Clay, J.M. Dramatic hydrodynamic and sedimentary responses in Galveston Bay and adjacent inner shelf to Hurricane Harvey. *Sci. Total Environ.* **2019**, *653*, 554–564. [[CrossRef](#)]
66. Burford, M.; Webster, I.; Revill, A.; Kenyon, R.; Whittle, M.; Curwen, G. Controls on phytoplankton productivity in a wet-dry tropical estuary. *Estuar. Coast. Shelf Sci.* **2012**, *113*, 141–151. [[CrossRef](#)]
67. Wetz, M.S.; Yoskowitz, D.W. An 'extreme' future for estuaries? Effects of extreme climatic events on estuarine water quality and ecology. *Mar. Pollut. Bull.* **2013**, *69*, 7–18. [[CrossRef](#)]
68. Huang, L.; Jian, W.; Song, X.; Huang, X.; Liu, S.; Qian, P.; Yin, K.; Wu, M. Species diversity and distribution for phytoplankton of the Pearl River estuary during rainy and dry seasons. *Mar. Pollut. Bull.* **2004**, *49*, 588–596. [[CrossRef](#)]
69. Lu, Z.; Gan, J. Controls of seasonal variability of phytoplankton blooms in the Pearl River Estuary. *Deep. Sea Res. Part II Top. Stud. Oceanogr.* **2015**, *117*, 86–96. [[CrossRef](#)]
70. Mallin, M.A.; Paerl, H.W.; Rudek, J. Seasonal phytoplankton composition, productivity and biomass in the Neuse River estuary, North Carolina. *Estuar. Coast. Shelf Sci.* **1991**, *32*, 609–623. [[CrossRef](#)]
71. Paerl, H.W.; Hall, N.S.; Peierls, B.L.; Rossignol, K.L. Evolving paradigms and challenges in estuarine and coastal eutrophication dynamics in a culturally and climatically stressed world. *Estuaries Coasts* **2014**, *37*, 243–258. [[CrossRef](#)]
72. Carstensen, J.; Klais, R.; Cloern, J.E. Phytoplankton blooms in estuarine and coastal waters: Seasonal patterns and key species. *Estuar. Coast. Shelf Sci.* **2015**, *162*, 98–109. [[CrossRef](#)]
73. Widdicombe, C.E.; Eloire, D.; Harbour, D.; Harris, R.P.; Somerfield, P.J. Long-term phytoplankton community dynamics in the Western English Channel. *J. Plankton Res.* **2010**, *32*, 643–655. [[CrossRef](#)]
74. Abreu, P.C.; Hartmann, C.; Odebrecht, C. Nutrient-rich saltwater and its influence on the phytoplankton of the patos lagoon estuary, Southern Brazil. *Estuar. Coast. Shelf Sci.* **1995**, *40*, 219–229. [[CrossRef](#)]
75. Quigg, A.; Claflin, N.; Kamalanathan, M.; Labonté, J.M.; Steichen, J.L. Response of a phytoplankton community in a subtropical estuary to a pulse disturbance driven by a combo hurricane and extreme rainfall event. *Estuaries Coasts* **2024**, *47*, 1032–1051. [[CrossRef](#)]

76. Thyng, K.M.; Hetland, R.D.; Socolofsky, S.A.; Fernando, N.; Turner, E.L.; Schoenbaechler, C. Hurricane Harvey caused unprecedented freshwater inflow to Galveston Bay. *Estuaries Coasts* **2020**, *43*, 1836–1852. [[CrossRef](#)]
77. Guan, X.; Gao, Z.; Huang, J.; Cao, C.; Zhu, K.; Wang, J. Speeding extreme cold events under global warming. *Environ. Res. Lett.* **2022**, *17*, 084012. [[CrossRef](#)]
78. Knutson, T.R.; McBride, J.L.; Chan, J.; Emanuel, K.; Holland, G.; Landsea, C.; Held, I.; Kossin, J.P.; Srivastava, A.; Sugi, M. Tropical cyclones and climate change. *Nat. Geosci.* **2010**, *3*, 157–163. [[CrossRef](#)]
79. Paerl, R.W.; Venezia, R.E.; Sanchez, J.J.; Paerl, H.W. Picophytoplankton dynamics in a large temperate estuary and impacts of extreme storm events. *Sci. Rep.* **2020**, *10*, 22026. [[CrossRef](#)] [[PubMed](#)]

Disclaimer/Publisher’s Note: The statements, opinions and data contained in all publications are solely those of the individual author(s) and contributor(s) and not of MDPI and/or the editor(s). MDPI and/or the editor(s) disclaim responsibility for any injury to people or property resulting from any ideas, methods, instructions or products referred to in the content.